Effect of sand as thermal damper integrated in flat plate water solar thermal collector

Amine T. Benhouia[*], Mohamed Teggar, Ahmed Benchatti

Laboratory of Mechanics, University of Laghouat, B.P. 37G, Laghouat 03000, Algeria

Corresponding Author Email: a.benhouia@lagh-univ.dz

ABSTRACT

An experimental study was carried out to evaluate the thermal performance of sand dune as storage material integrated in a flat solar thermal collector. The experimental apparatus is realized then installed on site. The parameter measured in this study is the temperature at different points of the collector. A graphic presentation shows the results obtained experimentally during the day of the test (winter period). The absorbing plate temperature reaches a maximum value of 97 °C and the layer of sand of 25 mm can ensure a storage of 20 minutes with a damping of thermal fluctuations of 5.2 °C. The amount of heat stored could replace the incident solar energy during the presence of clouds for 20 minutes.

1. INTRODUCTION

High radiation potential countries like Algeria are favorable for industrial as well as domestic solar thermal applications. Flat plate solar collectors are one of solar systems that can be used to harness the energy of the sun which is in turn transformed to thermal energy. Flat-plate solar collectors are largely used in thermal applications such as water heating or space heating.

Heat storage allows thermal energy to be used whenever needed especially when the source is intermittent or not available regularly. Solar thermal storage can be done with phase change (i.e. latent heat) [1] or with sensible heat. Different phase change materials have been used as storage materials like paraffin wax [2], such systems could present several advantages [3,4] among others reduction of the stagnation temperature and higher temperatures levels. However, these materials are expensive [5]. Thus, low cost and durable alternative storage materials can be effectively used such as fluids namely water or solids like concrete or sand [6]. Solar water heating using water as storage medium has been studied by Gertzos et al. [7]. Various heat exchanger designs were investigated by Al-Khalifajy et al. [8] and by Khalifa and Jabbar [9]. Solids like concrete and sand have good thermal storage qualities [10,11]. However, sand is largely used in solar integrated collectors; it is low cost and durable heat storage medium. In addition, sand is a local available material. Sathyamurthy et al. used sand as storage material in solar basin still [12]. Hazami conceived and realized a collector with concrete matrix as storage medium in order to ensure night solar greenhouse heating, solar integrated collector storage was experimentally studied [13]. The heating power was 1.5 KW of restored solar energy. Shoda et al. studied a solar collector of a glazed box partially filled with sand [14], polythene tubes are inserted in the sand at a certain depth. The authors analyzed the collector performance for constant flow rate of heat transfer fluid. Black colored sands are tested as collector absorber between double glazed water storage tank. High thermal efficiency of 70% was achieved with water tank temperature of 90°C [15].

However, the solar collector performances are directly affected by clouds or shades, direct solar radiation might drop significantly. Thus, storage systems can avoid this disturbance and ensure thermal energy delivery for a certain period. Consequently, radiation collection and thermal storage can be integrated in a simple compact structure integrated solar collector.

The present work is primarily aimed to analyze the effect of sand as storage medium on the performance of flat plate water thermal solar collector double glazed shown in Figure 1 with special focus on the radiation fluctuations. These fluctuations could be due to clouds or shade effect. Sand is used as a storage material because it is cheap and available.

Figure 1. Photograph of the experimental prototype

2. DESCRIPTION OF THE EXPERIMENTAL SET-UP AND TEST PROCEDURE
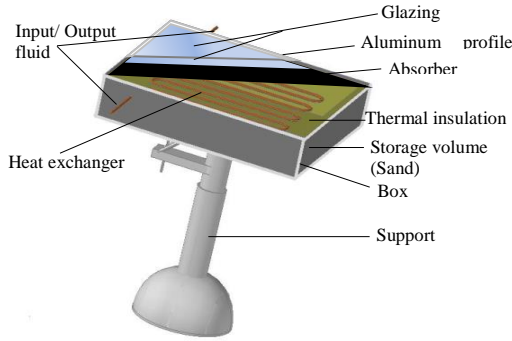
2.1 The experimental prototype

Figure 2. Schematic view of experimental prototype
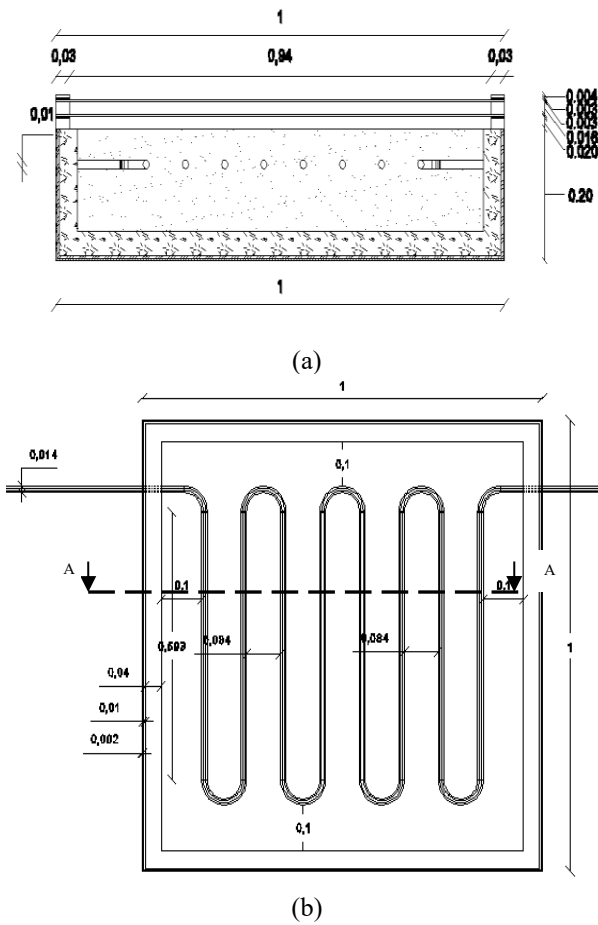

(a)

(b)

Figure 3. Schematic of the experimental prototype cross section (a); section A-A(b)

The experimental device shown in Figure 2 is a flat plate water solar thermal collector with an integrated storage system, it consists essentially of a double-glazing collector with a thickness of 3mm (the transmission coefficients 90%) which provides spaced forward insulation air gap with 16mm as shown in Figure 3-a. A gap of 20 mm is maintained from the glazing to the absorber of 1mm of thickness (the thermal conductivity and the specific heat of the absorbing plate are

equal to 0.81 W / m K and 0.880 kJ / kg K respectively). The storage volume is represented by the galvanized steel sheet box under the absorber, two insulation materials are used simultaneously to reduce thermal losses through the bottom and side walls, the glass wool as the first layer in direct contact with the inner walls of the box limited by the second layer of expanded polystyrene (the thermal conductivity and the specific heat of the glass wool and expanded polystyrene are equal to 0.035 W / m K, 0.034 W / m K and 0,28 W / kg K, 0.36 kJ / kg K respectively)then the storage volume is filled with a storage material with 150 mm of thickness.

The heat exchanger geometry contains copper serpentine tube, it is illustrated by Figure 3-b with inner diameter of 12 mm and outer diameter of 14 mm and length of 6230 mm and space between the tubes of 84 mm immersed inside the storage material.

The support is designed to hold the solar thermal collector when it is filled with the storage material, enable to be oriented ($\gamma = 360$ °) and inclined ($0 \leq \beta \leq 90$ °). The solar thermal collector is installed on a terrace whose geographical coordinates are:

Longitude $L = 2 ° 51'36''$
Latitude $\varphi = 33 ° 47'45''$
Altitude $l = 763$ m

The collector is oriented to the south with azimuth angle a = 0 ° and inclined with an angle $\beta \approx \varphi = 34$ ° [16].

From the T_9, T_{11} and T_{13} curves and from 8:10 to 9:00, a slight inversion phenomenon (clearly visible on the second depth $H_2 = 100$ mm) is reflected by the discharge period of the thermal energy stored during the day before the test without heat transfer fluid (HTF) flow, which ensures an energy compensation that lasts 60 minutes.
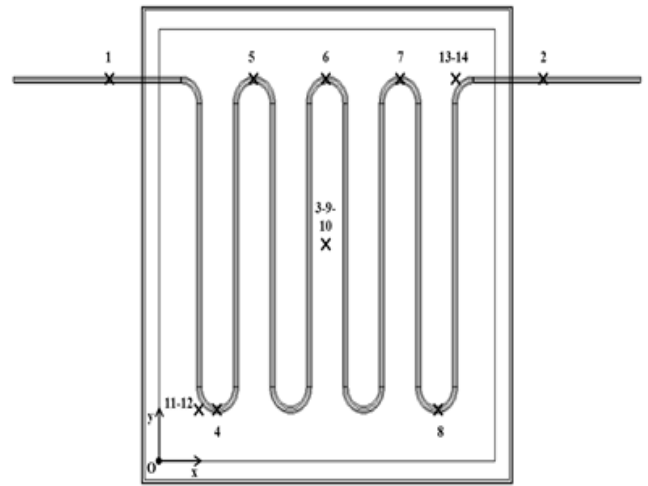

Figure 4. Position of thermocouples

Measurements start from sunrise to sunset by raising temperature every 10 minutes. Both Figure 4 and Table 1 shows the different points measurements in the solar thermal collector whose ambient temperature.

To measure the temperature, a digital thermometer and thermocouples type K are used, the operating range of the type K thermocouple is shown in Table 2 [17].

Table 1.

Table 1. Thermocouple coordinate system

Points	Thermocouples	x (m)	y (m)	z (m)
3	T_p	0.450	0.450	0.000
4	T_4	0.158	0.100	-0.050
5	T_5	0.254	0.800	-0.050
6	T_6	0.450	0.800	-0.050
7	T_7	0.646	0.800	-0.050
8	T_8	0.744	0.100	-0.050
9	T_9	0.450	0.450	-0.025
10	T_{10}	0.450	0.450	-0.100
11	T_{11}	0.100	0.100	-0.025
12	T_{12}	0.100	0.100	-0.100
13	T_{13}	0.800	0.800	-0.025
14	T_{14}	0.800	0.800	-0.100

Table 2. Operating range of type K thermocouple

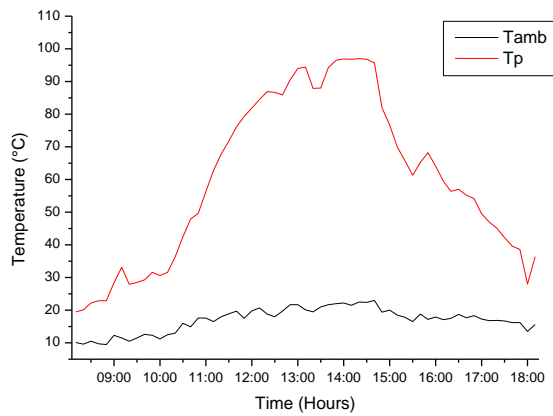| Type thermocouple	K
Composition	Chromel : 90% Ni, 10% Cr Alumel : 90% Ni, 2% Al, 2% Mn
Temperature range	0° to 275 °C
Special limits of error	±2,2 ° C or ±2%

3. EXPERIMENTAL RESULTS

Figure 5. Variation of the ambient and absorber temperatures vs time (January 29th)

Figure 5 shows both evolutions of ambient and absorber temperatures during the day of January 29. The ambient temperature varies over time for a minimum of 9.5 °C at 8:50 to maximum of 18.7 °C at 13:00. However, the absorber temperature increases and decreases with solar irradiance level and it reach its maximum of 97 °C at 14:20. A fluctuation observed during this day is explained by the clouds shadow effects that results in variations on the absorber temperature.

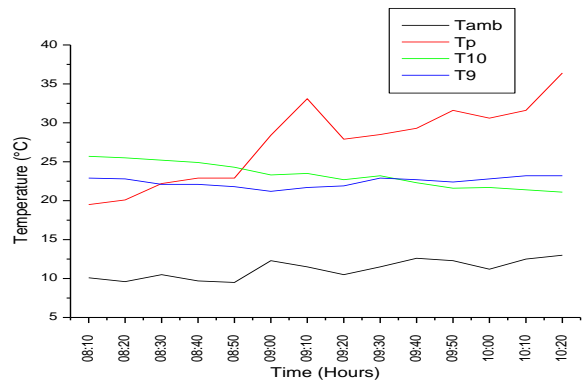Temperature evolutions of both the absorber plate and the storage volume (sand dune) at different depths from 8:10 to 18:10 are shown in Figure 6-a. We can distinguish two clusters of curves T_9, T_{11}, T_{13} and T_{10}, T_{12}, T_{14} which means that there is an isothermal sand layer for each cluster.

The mean sand temperature T_9, T_{11} and T_{13} on the first depth H_1= 25 mm reaches its maximum of 49 °C at 14:40 while the absorber plate temperature reaches its maximum of 97 °C at 14:20, i.e. a time difference of 20 minutes between the two peaks, so the heat energy received by the absorber plate stored in the sand will be restored with a delay time of 20 minutes or the signal emitted by the absorber plate lasts 20 minutes to cross a sand thickness of 25 mm, this time difference is called phase shift.
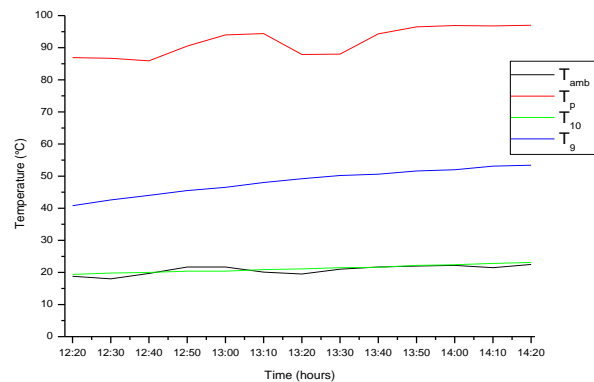
On the other hand for the second depth H_2=100mm, the time deviation between two peaks of absorber plate and sand temperatures T_{10}, T_{12} and T_{14} is quite extended 340 minutes compared to the absorber plate and the sand at depth of H_1 = 25 mm. Unlike upper sand layer, the phase shift of sand bottom layer is higher with lower thermal amplitude.
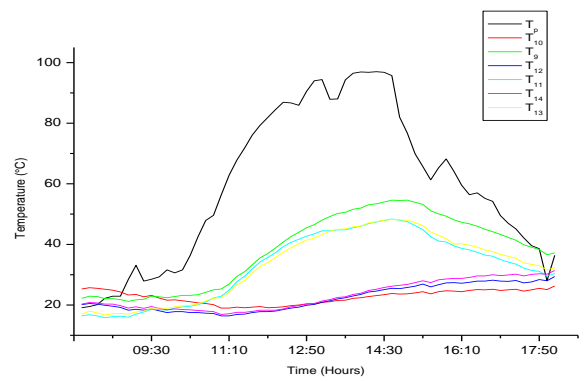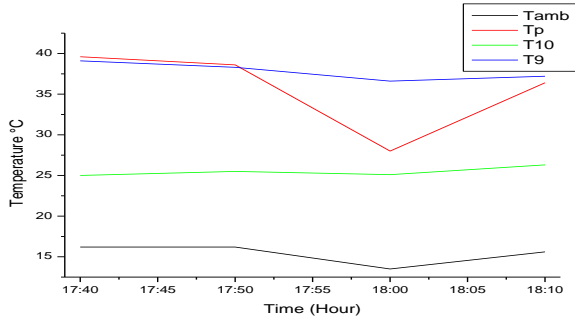

(a)

(b)

(c)

(d)

Figure 6. Temperature evolutions (a) the absorber and the storage; (b), (c) and (d) zoomed views of the data interval of January 29th
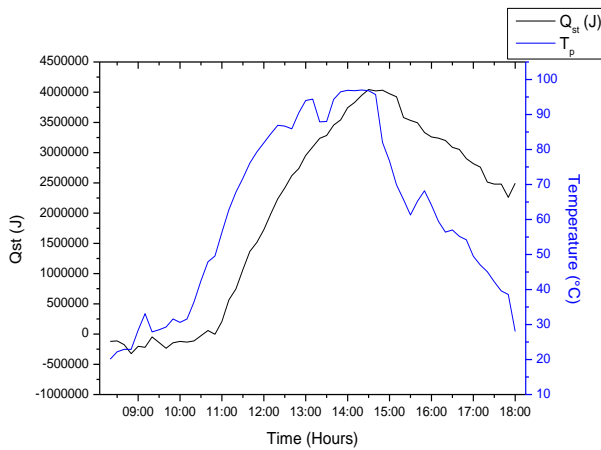

Figure 7. The evolution of thermal energy stored (accumulated) and the absorber plate temperature during the day of January 29th

The inversion phenomenon is explained by the fact that sand temperature decreases when the low temperature HTF flows across the heat exchanger until the equilibrium point at 9:00. After that, HTF temperature is affected by the absorbed energy which is higher than that of the day before.

A variation temperature between T_{11}, T_{13} and T_9 curves at both the beginning and the end of the day is due to the thermocouples' positions where T_{11} is placed in the inlet area of the heat exchanger and T_{13} in the outlet area, so the sand temperature near the inlet is slightly lowered by the HTF and vice versa at the outlet where the fluid recovers heat. On the other hand and between 11:20 and 13:00 where the absorber plate temperature increases gradually by 27 °C the sand temperature increases uniformly.

Figure 6-b shows a zoomed views of the data interval from 9:10 to 9:20, due to clouds, a temperature fluctuation is observed at the absorber plate temperature curve with a temperature deviation of 5.5 °C, this one lasts a time of 10 minutes to affect the sand upper layer with a decrease of 0.3 °C, so with damping of 5.2 °C. Whereas between 9:40 and 17:50 the temperature fluctuations seen in Figure 6-c appearing on the absorber plate temperature curve have no effect on the sand. At the end of the day (18:00), a temperature fluctuation due to the shading effect (caused by the experimental site) appearing in the temperature curve of the absorber plate seen in Figure 6-d with a temperature deviation of 10 °C, this disturbance appears immediately on

the sand but with a damping of 1.6 °C. It can be noticed that at the end of the day the sand thickness of 25 mm can offset the mismatch between solar energy availability and demand in this storage system.

The second bundle which represents the curves T_{10}, T_{12} and T_{14} for a depth of $H_2 = 100$ mm from the absorber plate, can be studied over two-time, first from 8:00 to 11:00, the sand temperature is decreasing slightly with a negative slope of 3 %, i.e. discharge period of the thermal energy stored the day before the test. And from 11:00 to the end of the operation, the sand temperature continues to increase in spite of the decrease in the absorber plate temperature, this represents the charging process.

As shown in Figure 7, we can distinguish the thermal energy stored process (calculated by the trapezoidal method) of our system (sand) versus time intervals.

From 8:20 to 10:40 the stored heat manifests by negative values, this is reflected by the discharge process [18], i.e. the energy stored the day before the test at closed cycles was restored for a period of 2 hours and 20 minutes. The fluctuations appear during the discharge process are due either to:

− The increase in the inlet HTF temperature (HTF source exposed to the environment) compared with that storage medium temperature (sand).

− The increase in the upper layer sand temperature compared to the lower one.

All this increases the heat stored, which reflects the short-term charge process.

At 10:40 the system reaches the thermal equilibrium ($Q_{st} = 0$) where the sand temperature is equal to that of HTF.

From 10:40 to 14:20 the stored heat increases despite the flow of the HTF across heat exchanger, this period represents the charging process.

The end of this period begins with a storage process where the stored heat remains nearly constant for almost one hour until 15:10, which means that the storage system (sand) keeps accumulating energy until the stagnation temperature.

Discharge process begins from 15:10 and continues until the end of operation, where the storage system (sand) restored the energy stored to ensure operation in the afternoon. The amount of heat stored during that day is 118727,4738 KJ.

5. CONCLUSIONS

From the experimental investigations the following results were obtained:

- The absorber is more sensitive to thermal shock which is due to cloudy periods, whereas that of the sand is very low which ensures the charge/discharge with damping of temperature deviations (drop) during the day.
- At the beginning of the day and for a sand thickness of 25 mm, the absorber temperature fluctuations of 5.5 °C appear after 20 minutes in sand with damping of 0.3 °C.
- In the middle of the day a temperature fluctuation of 5.5 °C doesn't appear on the sand, therefore sand can be used as damper that eliminates practically all the temperature drops due to cloudy periods or solar masks (Trees, buildings, mountains)

- Sand as thermal storage material can be used for a values temperature from 40 °C to 50 °C.
- The thermal behavior of sand layer H_1 = 25 mm is similar to the absorber except that the sand temperature decreases proportionally to the distance from absorber, thus it ensures the temperature variations damping associated to the environmental changes (mainly clouds).

REFERENCES

[1] Rabin Y, Bar-Niv I, Korin E, Mikic B. (1995). Integrated solar collector storage system based on a salt-hydrate phase-change material. Solar Energy 55(6): 435-444. http://dx.doi.org/ 10.1016/0038-092X(95)00074-2

[2] Chen Z, Gu M, Peng D. (2010). Heat transfer performance analysis of a solar flat-plate collector with an integrated metal foam porous structure filled with paraffin. Applied Thermal Engineering 30 (14-15): 1967-1973. http://dx.doi.org/10.1016/j.applthermaleng.2010.04.031

[3] Haillot D, Goetz V, Py X, Benabdelkarim M. (2011). High performance storage composite for the enhancement of solar domestic hot water systems Part 1: Storage material investigation. Solar Energy 85(5): 1021-1027. http://dx.doi.org/ 10.1016/j.solener.2011.02.016

[4] Haillot D, Nepveua F, Goetz V, Py X, Benabdelkarim M. (2012). High performance storage composite for the enhancement of solar domestic hot water systems: Part 2: Numerical system analysis. Solar Energy 86(1): 64-77. http://dx.doi.org/ 10.1016/j.solener.2011.09.006

[5] Sarbu I, Sebarchievici C. (2018). A comprehensive review of thermal energy storage, Sustainability 10(1). http://dx.doi.org/ 10.18690/978-961-286-052-3.14

[6] Badran AA, Yousef IA, Joudeh NK, Al Hamad R, Halawa H, Hassouneh HK. (2010). Portable solar cooker and water heater. Energy Convers Manag 51(8): 1605–1609. http://dx.doi.org/ 10.1016/j.enconman.2009.09.038

[7] Gertzos KP, Caouris YG. (2007). Experimental and computational study of the developed flow field in a flat plate integrated collector storage (ICS) solar device with recirculation. Experimental Thermal Fluid Science 31(8): 1133–45. http://dx.doi.org/ 10.1016/j.expthermflusci.2006.12.002

[8] AL-Khaffajy M, Mossad R. (2013). Optimization of the heat exchanger in a flat plate indirect heating integrated collector storage solar water heating system. Renewable Energy 57: 413–421. http://dx.doi.org/ 10.1016/j.renene.2012.11.033

[9] Khalifa A, Abdul Jabbar RA. (2010). Conventional versus storage domestic solar hot water systems: a comparative performance study. Energy Conversionand Management 51(2): 265-270. http://dx.doi.org/ 10.1016/j.enconman.2009.09.021

[10] Nieuwoudt MN, Mathews EH. (2005). A mobile solar water heater for rural housing in Southern Africa. Build Environ 40(9): 1217–1234. http://dx.doi.org/ 10.1016/j.buildenv.2004.11.024

[11] Kumar R, Rosen MA. (2010). Thermal performance of integrated collector storage solar water heater with corrugated absorber surface. Appl Therm Eng. 30(13): 1764-1768. http://dx.doi.org/ 10.1016/j.applthermaleng.2010.04.007

[12] Sathyamurthy R, Nagarajan PK, Edwin MA, Madhu B, El-Agouz SA, Ahsan A, Mageshbabu D. (2016). Experimental investigations on conventional solar still with sand heat energy storage. International Journal of Heat and Technology 34(4): 597-603. http://dx.doi.org/ 10.18280/ijht.340407

[13] Hazami M, Kooli S, Farhat A, Belghith A. (2005). Performance of a solar storage collector. Desalination 183(1-3): 167-172. http://dx.doi.org/ 10.1016/j.desal.2005.03.033

[14] Sopian K, Syahri M, Abdullah S, Othman MY, Yatim B. (2004). Performance of a non metallic unglazed solar water heater with integrated storage system. Renew Energy 29: 1421-1430. http://dx.doi.org/ 10.1016/j.renene.2004.01.002

[15] Taheri Y, Ziapour BM, Alimardani K. (2013). Study of an efficient compact solar water heater. Energy Conversion and Management 70: 187-193. http://dx.doi.org/ 10.1016/j.enconman.2013.02.014

[16] Duffie, Beckman. (1991). Solar engineering of thermal processes. In: John Wiley, Son Inc. (eds), NY.

[17] Manual on the Use of Thermocouples in Temperature Measurement: 4th Edition. (1993). American Society for Testing and Materials. R M Park (ed), Philadelphia, USA.

[18] Ibrahim D, Marc AR. (2011). Thermal energy storage systems and applications. In: Wiley J, Son Ltd, Canada.

NOMENCLATURE

a	Solar azimuth angle, degrees
L	Longitude, degrees
l	Altitude, m
Q	Energy, J
T	Temperature, K

Greek symbols

β	Collector declinaison, degrees
γ	Collector slope, degrees
φ	Latitude, degrees

Subscripts

amb	ambient
ab	absorber
p	plate
st	store